Chapter 3: MATERIALS AND EXPERIMENTAL TECHNIQUES

3.1 INTRODUCTION

The experimental investigations included the following:

- Scanning Electron Microscopy (SEM-EDX) analysis and X-ray analyses (XRF and XRD) for surface characterisation of slabs (stainless-steel type 304),
- Decarburisation of powder mould flux at 600ºC in air in a muffle furnace followed by chemical analyses (XRF, ICP-AES and LECO elemental analysis for carbon and sulphur),
- Contamination of the upper steel surface with a paste prepared by mixing alcohol with decarburized powder flux, before reheating,
- Scale growth under reheating conditions, using large samples to avoid edge effects,
- Scanning Electron Microscopy (SEM-EDX) and X-ray diffraction for characterisation of the oxide layers,
- X-Ray photoelectron spectroscopy (XPS) analyses were used to determine the oxidation state of chromium in the removed scales,
- High-pressure water descaling of hot samples,
- Scanning Electron Microscopy (SEM-EDX) and X-ray diffraction for characterisation of the oxide layers and morphology at the interface after descaling,

Preliminary high temperature reheating trials were done on the contaminated and non-contaminate slabs under reheating conditions in order to test the water level in the gas atmosphere and to assess the melting of powder flux on the slab top surface under reheating conditions.

3.2 SAMPLE SIZE AND SAMPLE COMPOSITION

SEM-EDS analysis was used for chemical elemental analysis of slab and hot rolled samples used for reheating following by descaling, and XRF, ICP-AES and LECO analyses were used for quantitative analysis of decarburized powder fluxes used to

contaminate the samples. XRF analysis was used to determine powder flux metallic oxide components, ICP-AES to determine fluorine and phosphorus, and carbon and sulphur were determined by combustion methods (LECO). The average chemical compositions of stainless steel and decarburised industrial mould fluxes used during this investigation are given in table 3.1 below.

In order to determine the effects of mould flux type on descaling and how the differences in mould flux composition affect the scale structure, synthetic mould fluxes were also prepared. Table 3.2 gives the composition of these synthetic mould fluxes.

TABLE 3.1: Stainless steel composition (mass percentages, balance iron) and decarburized mould flux compositions (mass percentages).

Steel		**Mould fluxes**			
Elements	[%]	Species[%]	Type 832	Type RF1	Type 810
Cr	18.16	SiO_2	35.92	33.97	34.10
Ni	8.09	CaO	32.53	38.98	35.34
Mn	1.305	Al_2O_3	5.92	7.32	6.98
Si	0.40	F	3.16	3.32	5.35
Mo	0.14	Na_2O	18.43	13.11	13.34
V	0.12	Fe_2O_3	0.55	1.46	1.52
Cu	0.09	MgO	2.6	0.96	1.43
C	0.044	TiO_2	0.19	0.14	0.30
N	0.050	MnO	0.057	0.035	2.81
Co	0.03	K_2O	0.13	0.55	0.17
P	0.022	P	0.053	0.038	0.06
Ti	0.01	Cr	0.073	0.005	0.015
O	0.0080	Ni	0.002	0.001	0.011
Al	0.004	V	0.007	0.002	0.017
S	0.0033	Zn	0.07	0.019	0.019
Nb	0.003	Sr	0.014	0.097	0.023
B	0.001	CaO/SiO_2	0.905	1.147	1.036

TABLE 3.2: Synthetic mould flux compositions (mass percentages)

Mould Flux	**CaO**	**SiO_2**	**CaF_2**	**Na_2O**
SMF1	40%	40%	20%	-
SMF2	40%	40%	-	20%
SMF3	50%	50%	-	-

The steel samples were cut to size from hot rolled plate using a band saw as well as a fixed abrasive disc cutter. Since stresses are developed at the edges and corners during scale growth, samples had large lengths and widths in comparison to the scale thickness (which could be as high as 0.5cm for longer reheating times). The steel samples were typically around 45mm x 45mm x 15mm large. The sample corners were bevelled away, to allow the samples to hang with their larger dimensions horizontal inside a tube furnace (to avoid mould flux dripping from the upper sample surface, where the flux was placed). Grooves, 1.5mm deep, on each side of the sample, served to secure the sample with Kanthal wire to a mullite rod. Figure 3.1 below shows a sketch of the sample, Kanthal wire and the mullite rod used to hang the sample in the furnace. Figure 3.15 on page 48, shows a photograph of a sample in the descaling device.

The stainless steel samples used in this investigation were slabs of continuous casting and plant-pickled plate samples (15mm thick), and were hence only degreased (with alcohol) before scaling. After reheating in gas atmosphere, the surface of the slabs and scale were characterised by SEM and X-ray analysis.

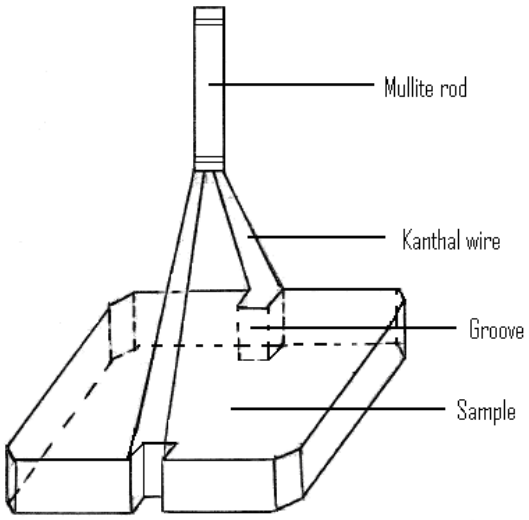

FIGURE 3.1: Sketch of the samples used during the experimental runs (not drawn to scale).

Casting powder (flux) was decarburised at 600ºC for 15 hours in air in a muffle furnace before the flux was applied to the steel surface.

Three types of industrial mould fluxes were used in this investigation to growth scale on 304 slab; type 832, STSP 810 (Stollberg) and RF1 (Syntherm). Synthetic mould fluxes SMF1, SMF2 and SMF3 were also used.

X-ray diffraction (XRD) of decarburized type RF1 flux (generally used for stainless steel type 321) revealed the following phases: $Ca_4Si_2O_7F_2$ (Cuspidine), $Na_2Al_2Si_2O_8$ (Nepheline) and CaF_2 (Fluorite). LECO analysis gave 0.1% carbon and 0.62% sulphur in this flux.

3.3 EXPERIMENTAL SET- UP FOR SLAB REHEATING AND DESCALING

3.3.1 Reheating Experimental Set-up used to Growth the Scale

The experimental set-up used to simulate industrial reheating conditions is shown in figure 3.2 below.

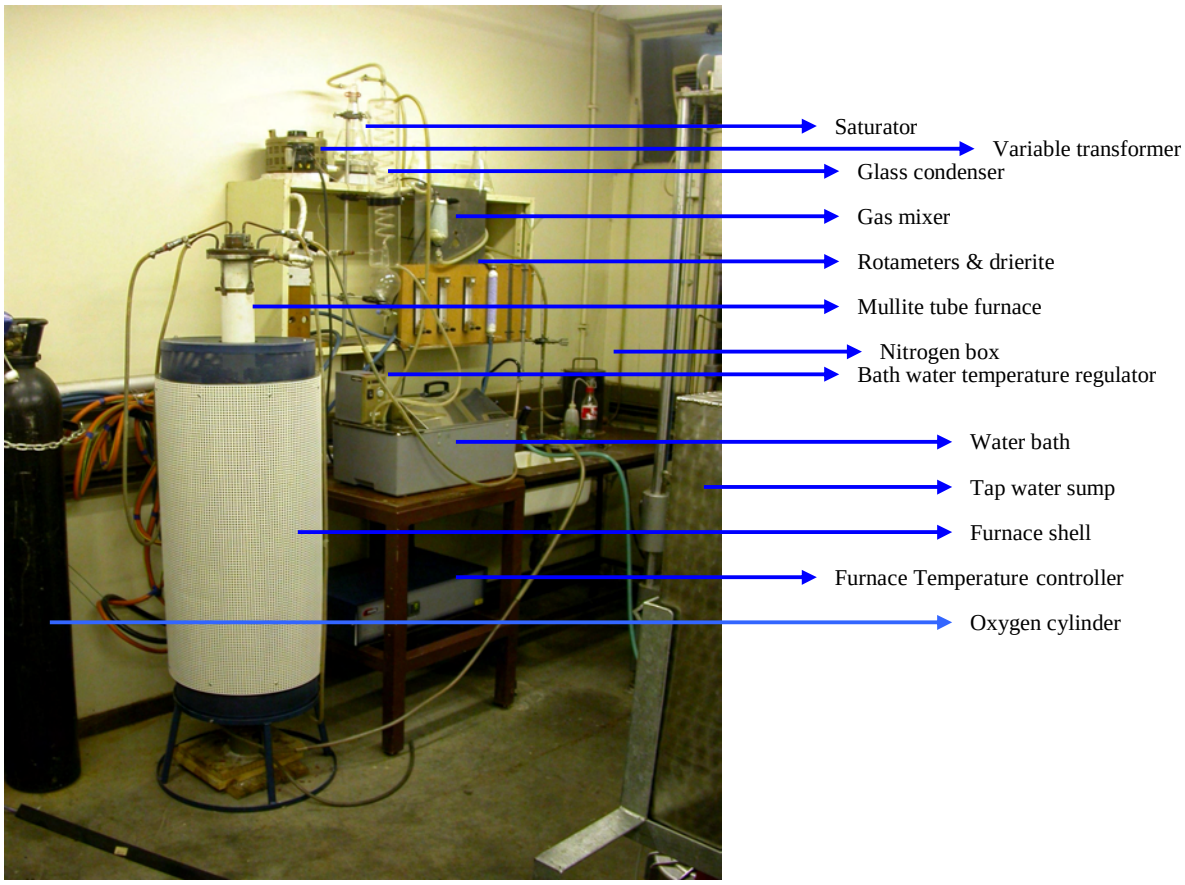

FIGURE 3.2: Photograph of the reheating experimental set-up

3.3.2. Gas Mixing System

The gas system was chosen to simulate the combustion product of methane (CH_4) in air with 3% or 4% excess free oxygen, that is, the gas contained CO_2, O_2, N_2 and water vapour. The gas flow rate was chosen to produce similar mass transfer conditions (which depend on the Reynolds number) to industrial furnaces. The total gas flow rate was equal to 5Ndm^3/min. The gases, CO_2, O_2, N_2, were chemical pure

with the minimum purity of both oxygen and nitrogen equal to 99.5% and that of carbon dioxide 99.0%.

The three gas lines were then joined before the gas mixer. The flow rate of each gas was measured and controlled by the rotameters which were calibrated by means of a bubble-meter. Calibration was done in order to ensure that accurate amounts of gas are flowing through the reactor. To check gas flow rates, the gases were allowed to flow from the regulator on the gas cylinder through the rotameter to a graduated cylinder filled with liquid soap up to the gas inlet level. By passing the gas through the graduated cylinder, the soap produced bubbles which moved upward and exited through the outlet gas. This allows the gas bubble to travel through a specific length of the cylinder. From the inside diameter of the cylinder, the volume travelled by the gas during a specific interval was determined and so the flow rate was calculated as the ratio volume-time take by the gas to travel a certain distance in the graduated cylinder at the ambient temperature (25ºC) and atmospheric pressure of Pretoria (0.865 atm). The ratio was evaluated at a certain setting on the rotameter. The sketch of the system used to calibrate the gas flow rate is shown in figure 3.3 below.

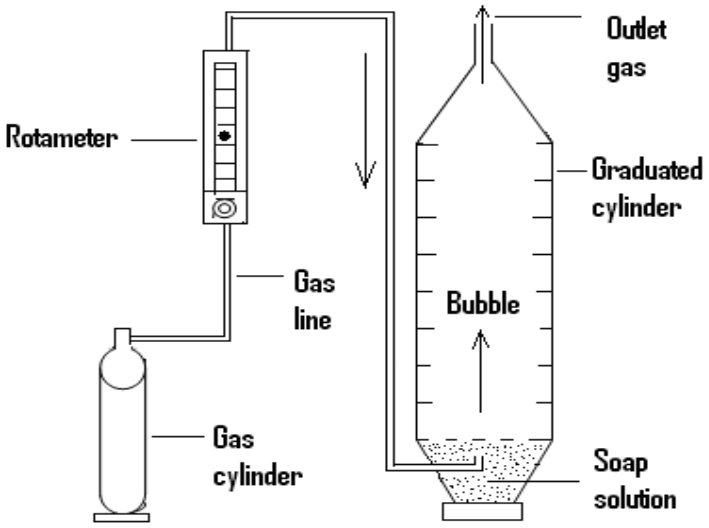

FIGURE 3.3: Schematic representation of the apparatus used to calibrate the gas flow rate (not drawn to scale).

Rotameter setting was determined by plotting gas flow rate versus rotameter reading. Correlations fitted to these results were used to calculate the position of the float in the rotameter for a specific flow rate.

The inline calibration of the rotameters was essential to ensure that the exact flow of the gas mixture was maintained, because a back pressure in the gas line would definitely affect the flow rate. The gas mixing set-up is shown schematically in figure 3.4. The appendix 1 details the process of rotameter calibration and settings

The gas mixer is a glass cylinder filled with glass beads to give turbulent flow of gases and proper mixing of the gases. After the gas mixture left the mixer, it then entered the saturator, which was filled with water kept near its boiling point.

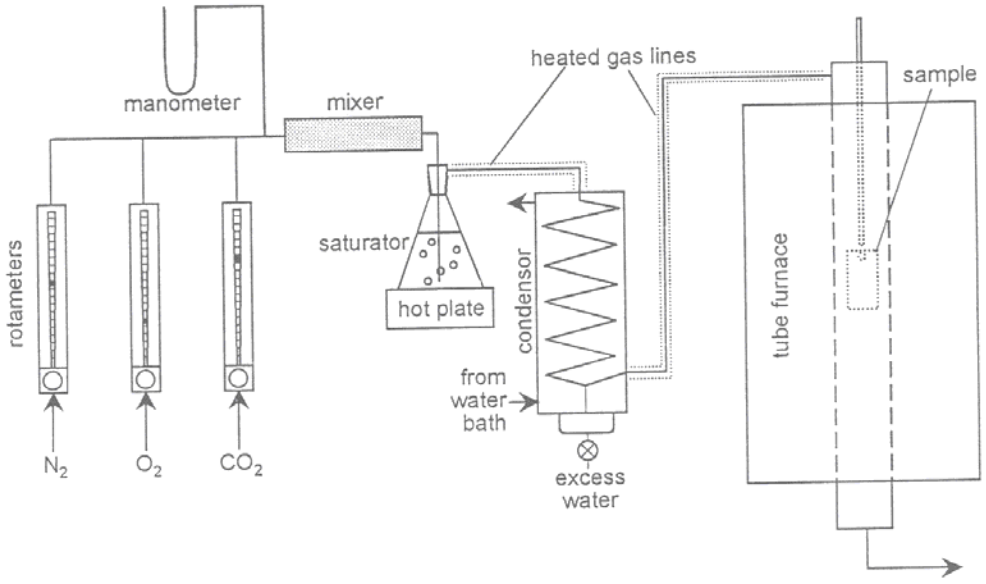

FIGURE 3.4: Experimental configuration used to grow scale in reheating furnace (Pistorius *et al.*, 2003).

Passing the gas through the saturator loads the gas with water vapour. By passing the mixture trough a temperature-controlled glass condenser, the excess water was removed and periodically drained off through the outlet at the bottom of the condenser.

A schematic representation of the temperature-controlled condenser is shown in the figure below:

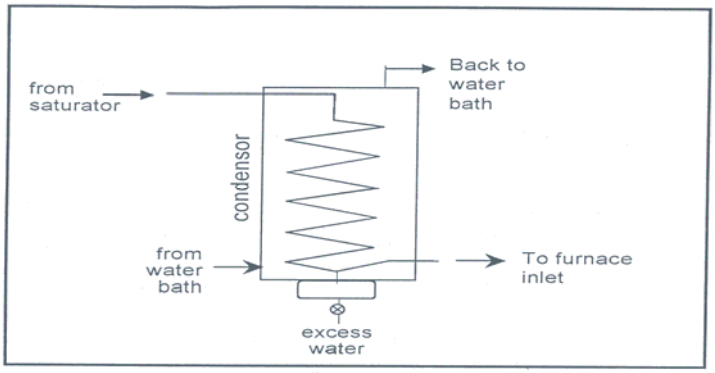

FIGURE 3.5**:** Schematic representation of temperature-controlled glass condenser (Pistorius *et al.*, 2003).

The temperature of the water circulating in the outer section of the condenser was maintained at 60ºC. This temperature control was accomplished by using a water bath. Between the exit of the condenser and the furnace inlet, a three-way brass valve was fitted. All the connections between the water saturator and the furnace were heated by using heavy insulated heating tape with a knitted Fibrox covering (Barnstead Thermolyne). The variable transformer controlling the heating tape temperature was set at 130 V so as to ensure that the temperature of the heating tape was approximately 80ºC. All connections between the regulators and the condenser were carried out using silicone rubber tubing, whereas those between the three-way valve and the furnace were done by using PFA-tubing. The PFA-tubing was used because its hardness made wrapping the heating tape around it easier. The gas mixture was checked to make certain it contained the correct amount of water vapour. To do this, the gas outlet at the bottom of the furnace was connected to a pre-weighed drierite (anhydrous $CaSO_4$) column, which was weighed again after the experiments. The amount of water that was absorbed by the drierite was established by the difference in weight. The theoretical and measured values of the water vapour in the gas mixture were 18.54g and 19.88 g (See Appendix 2).

3.3.3 Furnace Set-up

Reheating experiments was carried out in a vertical tubular furnace with a mullite working tube. The dimensions of the tube were 150 cm length × 9.0 cm O.D. × 7.6cm I.D. The inside diameter of 7.6 cm allowed for oxidation of samples with the following typical dimension: width = 45 mm, length = 45 mm and thickness = 15mm.

The furnace temperature was controlled by a Eurotherm 902P controller / programmer using a thermocouple that was positioned next to the furnace tube, close to the hot zone.

A schematic representation the furnace assembly is shown in figure 3.6.

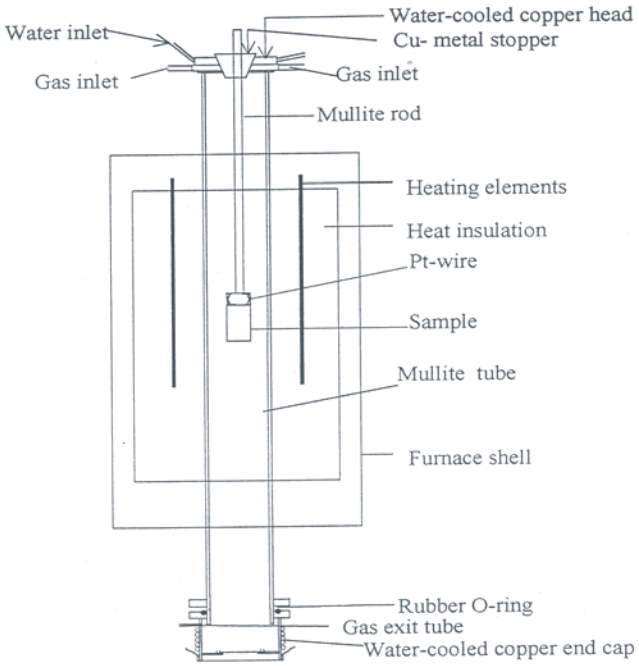

FIGURE 3.6: Schematic representation of furnace assembly (Pistorius *et al.*, 2003).

The exact position of the hot zone was measured by placing a hand-held type R (Pt-13% Rh) thermocouple at various depths in the furnace tube. The temperature profiles for programmed temperatures 1250°C and 1300°C are shown in figure 3.6.

The reference point from which the depth was measured was the top of the working tube.

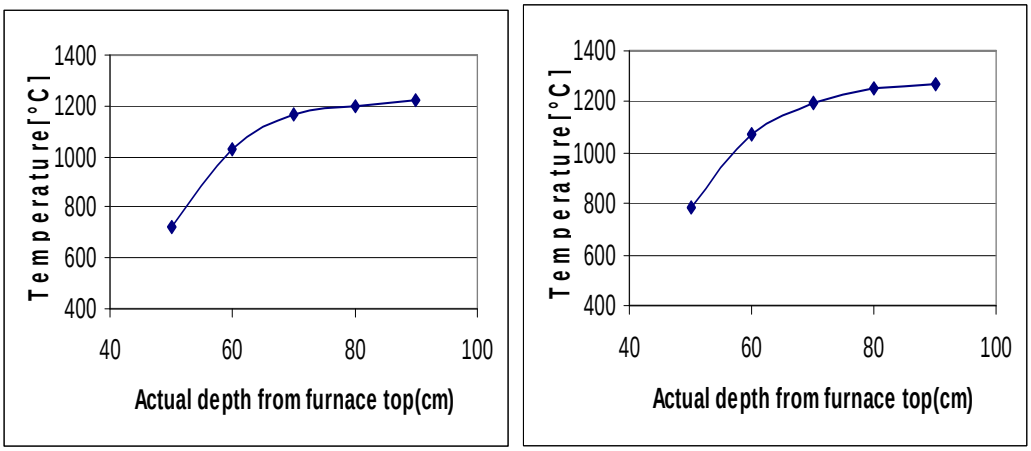

FIGURE 3.7: Temperature profile at programmed furnace temperatures of 1250°C and 1300°C

The measured temperature in hot zone as a function of programmed furnace temperature is shown in the chart below:

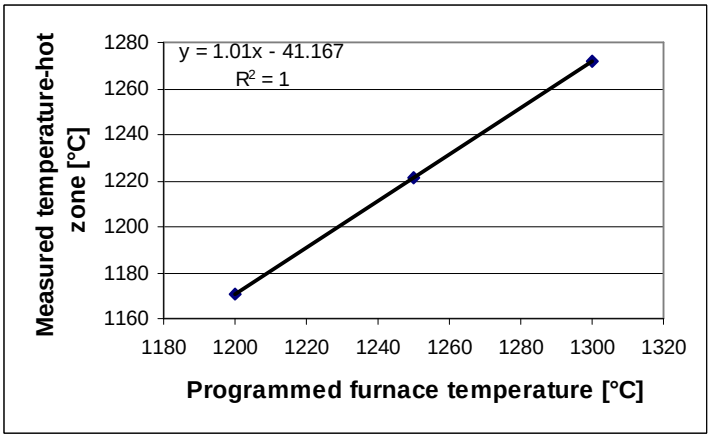

FIGURE 3.8: Measured temperature in hot zone versus programmed furnace temperature at a depth of 90cm below furnace top.

The average temperature of the hot zone measured with the hand–held thermocouple was within 30ºC of that indicated by the furnace controller.

The mullite furnace tube (9 O.D. x 7.6 cm I.D. x 150 cm lengths) was fitted with water-cooled copper heads at both ends. The bottom fitting extended below the mullite tube and was sealed with an O-ring lubricated with high temperature vacuum

grease. The upper end cap was sealed to the open flat end of the tube, sealing on a rubber gasket between the tube and the fitting. A steel bracket attached to the furnace tube exerted pressure on the gasket. Braided tubing was used for connecting the cooling water inlet and outlet to the furnace. Quick-connect couplings were used to ensure that the cooling water tubes could easily be removed from the copper-end cap before removal of the sample for descaling.

3.3.4 High Pressure Hydraulic Descaling Set-up

Immediately after the scaling period, the samples were removed from the furnace and subjected to hydraulic descaling; cooling of the sample can lead to ineffectiveness of the descaling (Sheppard & Steen, 1970).

The experimental laboratory descaling unit is shown in figure 3.9.

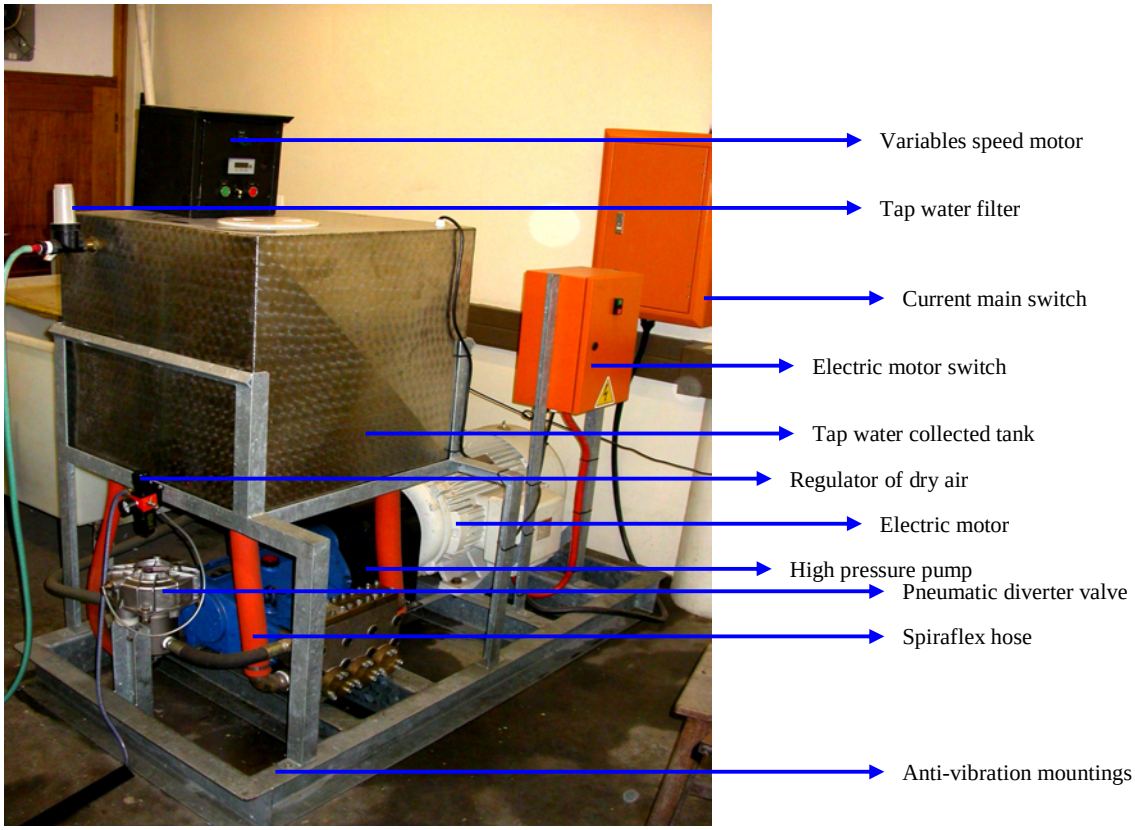

FIGURE 3.9: Photograph of the descaling assembly: pump and feed tank

3.3.4.1. Description of High Pressure Water Descaling Set-up

A schematic drawing of the descaling system is shown in Figure 3.10; the letters in the description below refer to the letters identifying different parts in the figure. The high pressure pump (J) was driven by a 55kW electric motor (L), Tap water (N) was filtered (K) and collected in a 400 litre sump (H) before each descaling run. Both pump and motor were fitted to a base frame mounted on anti-vibration mountings. The pressure/flow was adjusted via a pneumatic diverter valve (F). Dried compressed air from a regulator (G) actuated the diverter valve. High pressure water was piped from the pump unit to the hot steel samples through a 54 mm bore Spiraflex hose filled with two digital transmitters type 2020 TG (D) on either side of an orifice plate, which allowed the measurement of pressure and water flow rate. From the Spiraflex hose pipe water was sprayed through a single inclined nozzle (C). The nozzle was fixed to a steel rod by means of a coil-spring so that the nozzle height could be adjusted vertically; the nozzle was angled (15°, from vertical axis) [See figure 3.11]. The nozzle (LECHLER 694.726 with elliptical orifice) produced a water jet spray angle of 26° at 13.90 MPa. The vertical spray height was 96mm.

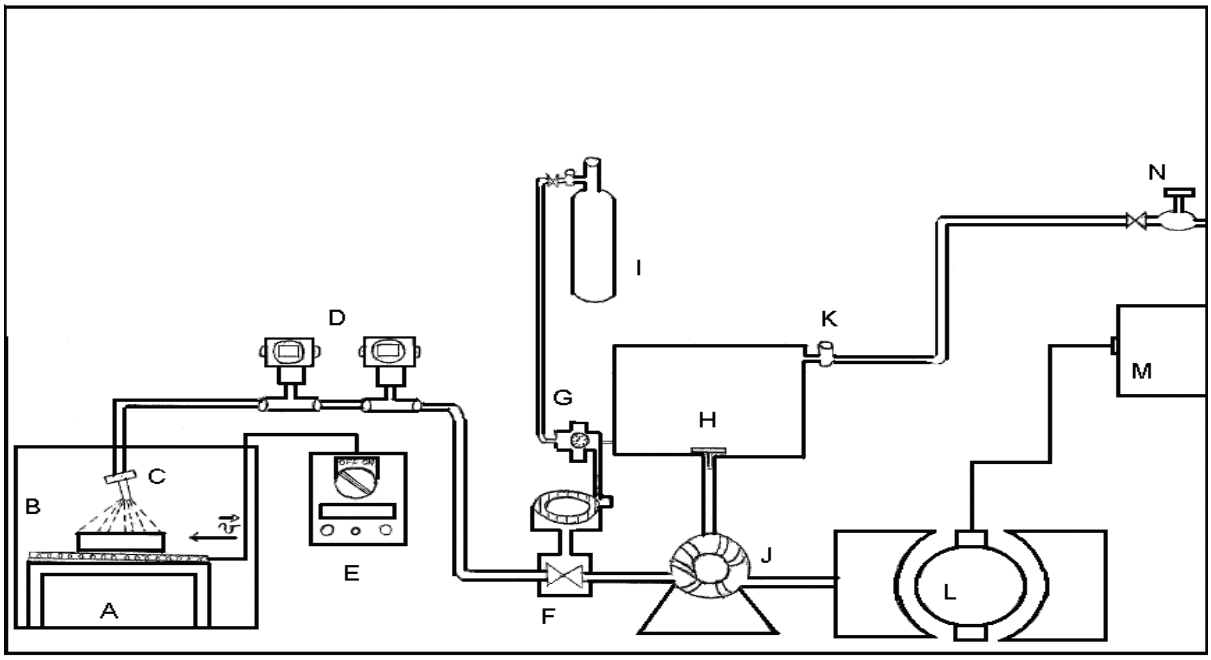

FIGURE 3.10: Schematic representation of the laboratory hydraulic descaler (not drawn to scale).

The hot steel sample for descaling was placed on a carriage (B) which moved underneath the descaling nozzle, by means of two parallel stainless steel runners. A variable speed motor and pulley (E) were used to propel the sample carriage (the speed was 0.8 m/s for stainless steel type 304). Upon descaling the water and scale fell into, and were collected in a 1050 litre holding tank (A).

3.4 EXPERIMENTAL RUN

3.4.1 Basic Matrix of Experiments

The experimental conditions for scale characterisation and for scale removal are shown in table 3.3 and 3.5 respectively.

Reheating for scale characterisation was performed at 1250ºC and 1280ºC using 3% and 4% free oxygen for 2, 3, 5 and 6 hours. Under these conditions, we expected to get a thick scale which should allow study of scale appearance, morphology and composition.

Descaling conditions were around 0.8m/s for the descaling speed, in line with the plant practice. Descaling vertical spray height was 96 mm and descaling water flow rate varied between 54 l/min and 66 l/min to get maximum impact pressures between 1.45 and 2.16 N/mm^2. The maximum impact pressure at the plant is 1.45 N/mm^2.

The basic outline of experiments is shown in table 3.3 below:

TABLE 3.3: Experimental matrix of reheating for scale characterisation

Temperature (ºC)	**% O_2**	**Reheating time (h)**
1250	3&4	2, 3, 5 & 6
1280	3&4	5 & 6

The experimental gas flow rate and rotameter settings used during reheating in 3%O_2 and 4% O_2 are given below:

TABLE 3.4**:** Gas flow rate and rotameter settings at 1 atmosphere for 3% and 4% free O_2 in the gas atmosphere

3%O_2	**Gas calibration & setting**	
	Gas flow rate	**Rot. setting**
N_2	3.92 dm^3/min	3.42 dm^3/min
O_2	0.16 dm^3/min	0.14 dm^3/min
CO_2	0.44 dm^3/min	0.32 dm^3/min

4%O_2	**Gas calibration & setting**	
	Gas flow rate	**Rot. setting**
N_2	3.91 dm^3/min	3.41 dm^3/min
O_2	0.22 dm^3/min	0.19 dm^3/min
CO_2	0.41 dm^3/min	0.33 dm^3/min

The basic outline of experiments is shown in Table 3.5 below:

TABLE 3.5: Experimental matrix for scale removal and descaling assessment

T[° C] Reheating	**% O_2 Reheating**	**Time[hr] Reheating**	**Descaling Speed [m/s]**	**Descaling Flow rate[l/min]**	**Descaling Spray height [mm]**
1250	3 & 4	2 - 6	0.8	54.40 - 65.96	96
1280	3 & 4	2 - 6	0.8	54.40 - 65.96	96
1300	3 & 4	2 - 6	0.8	54.40 - 65.96	96

Both descaling and reheating conditions were varied, but for the contaminated samples it was found that descaling effectiveness mainly depended on reheating conditions. Fifty-four experiments were done in total of which twenty-seven were for scale oxide characterisation, and twenty-seven were reheating followed with high pressure water spray for slab descaling. These were done under variable and constant reheating and descaling conditions.

3.4.2 Reheating Experiments

The temperature during reheating was generally monitored and controlled by means of the furnace thermocouple. However, in two runs an additional thermocouple was spot-welded to the sample surface, and it was found that the sample temperature was generally within 8°C of the furnace temperature.

The furnace was heated to the reheating temperature, and then the sample was placed in the furnace before starting gas flow. For both contaminated and uncontaminated samples, the temperature dropped (by about 15°C) when the sample was introduced and the gas flow was started - due to the opposing effects of the quenching effect of the introduction of non-preheated gas, and the exothermic scaling reaction. After approximately 8 minutes of the scaling, the temperature again reached its nominal value. At the end of the scaling period, the sample was removed from the furnace in a rapid and reproducible way, to avoid cooling before descaling.

3.4.3 Descaling Experiments

As mentioned earlier, the water pressure/flow during hydraulic descaling was monitored and controlled by a pneumatic valve.

Prior to descaling, the descaling water flow rate and system pressure were calibrated and monitored. The calibration procedure was as follows:

i. Set the pneumatic regulator valve pressure,
ii. Measure the level of water in the sump and the tank,
iii. Switch on the pump and use a stop watch to measure the water level variation in the tank and the sump,
iv. Read the corresponding pressures at the two digital transmitters,
v. Plot the curve of water flow rate versus regulator pressure and the curves of pressure at the first and the second transmitters versus the regulator pressure.

The photograph in figure 3.11 gives a view of the inside of the descaling tank.

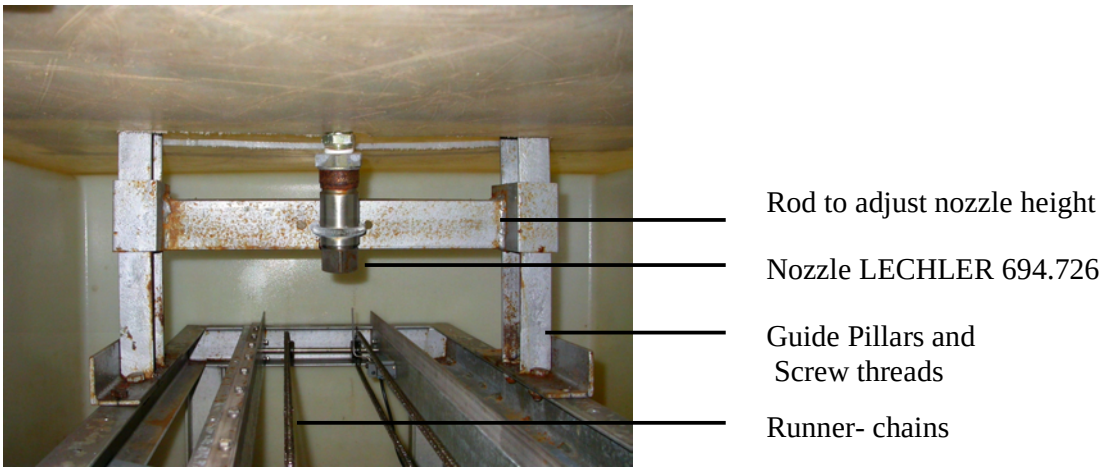

FIGURE 3.11: Descaling tank which shows the descaling nozzle, the adjustable spray height and the descaling speed chain.

The capacity of the high pressure pump used was 108 l/min of maximum water flow rate and 30 MPa pressure.

Table 3.6 below gives the descaling system pressure and water flow rate monitoring and calibration.

TABLE 3.6: Descaling system pressure and water flow rate calibration and setting

Pr	**P1s**	**P1**	**P2s**	**P2**	**Qt**	**Qb**	**ΔPs**	**ΔP**	**Qav**
[kPa]	[%]	[MPa]	[%]	[MPa]	[l/min]	[l/min]	[%]	[MPa]	[l/min]
49	13.9	8.3	13.7	8.2	40.4	44.3	0.12	0.072	42.4
137	26.0	15.6	25.8	15.5	55.2	57.6	0.18	0.108	56.4
196	38.6	23.1	38.3	23.0	66.6	70.9	0.225	0.135	68.8
245	43.4	26.0	43.1	25.9	71.3	72.4	0.24	0.144	71.9

Pr (kPa) dry air regulator pressure
P1s (%) setting pressure at the first digital transmitter
P1 (MPa) pressure at the first digital transmitter
P2s (%) setting pressure at the second digital transmitter
P2 (MPa) pressure at the second digital transmitter
ΔPs (%) variation of the setting pressure between two digital transmitters
ΔP (MPa) variation of the pressure between two digital transmitters
Qt (l/min) water flow rate measured at the first transmitter
Qb (l/min) water flow rate measured at the second transmitter
Qav (l/min) average water flow rate

Figures 3.12, 3.13 and 3.14 give the laboratory descaling calibration and settings curves. Figure 3.12 gives the water system pressure versus the pressure of dry air (read at the pressure regulator), Figure 3.13 gives the water flow rate at the descaling nozzle versus the air pressure (read at the pressure regulator), and Figure 3.14 gives

the descaling water flow rates as a function of the difference in pressure between the second and the first transmitters

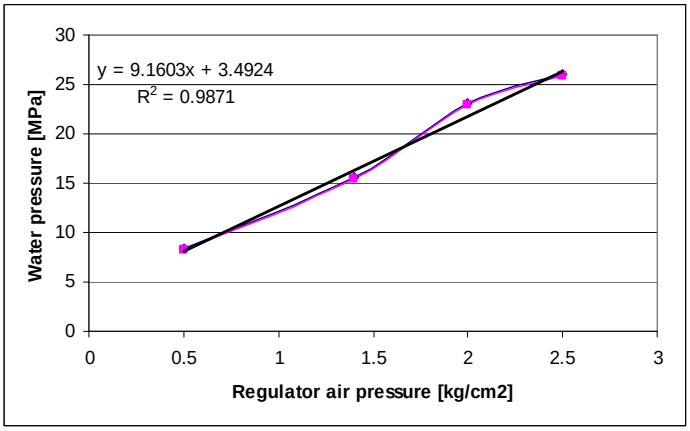

FIGURE 3.12: Water system pressure versus the regulator air pressure

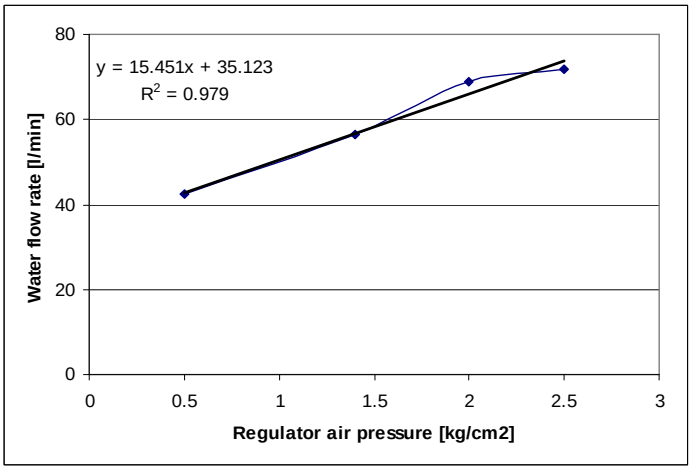

FIGURE 3.13: Descaling water flow rate versus the regulator air pressure

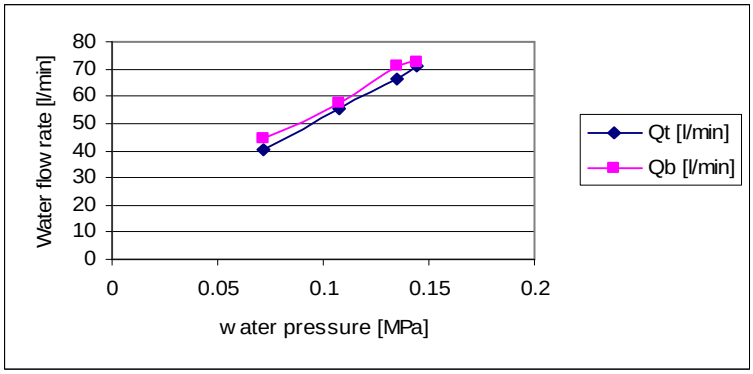

FIGURE 3.14: Descaling water flow rate versus the difference in pressure between the second and the first transmitter.

Two or three minutes before high pressure descaling the motor was started and the regulator air pressure manually set to the value which corresponded to the desired water flow rate. The hot sample was placed in the carriage and (quickly, and in a reproducible way) the motor pulley was started to move the hot sample at the require velocity until it reached the descaling nozzle. For a sample reheated at 1280°C, it was found that the sample temperature just before high pressure hydraulic descaling was approximately 1185°C. Just after descaling both the pump and the motor pulley were stopped. Once cold, descaled samples and the removed scales were collected for visual observation and analysis. The photograph on figure 3.15 shows a sample placed on the sample carriage.

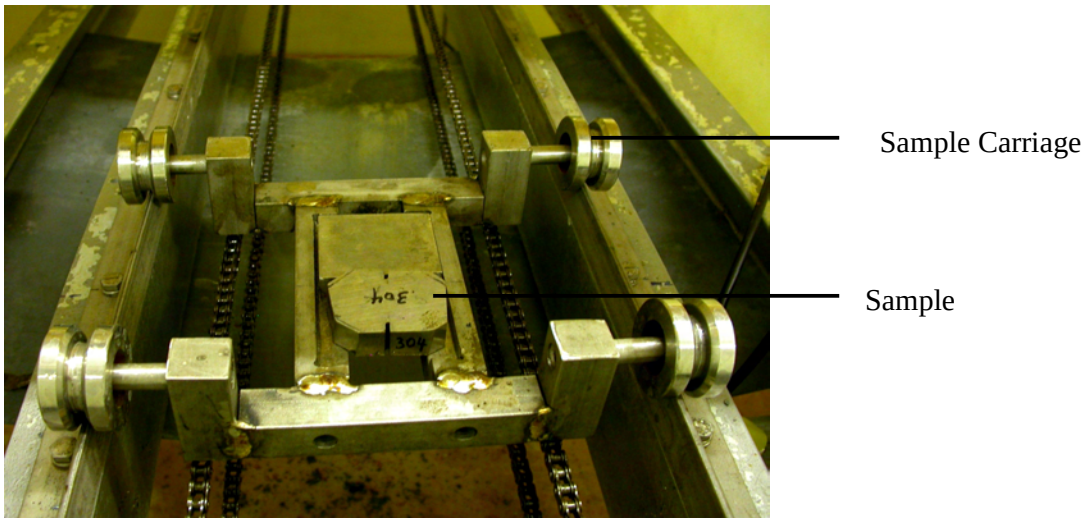

FIGURE 3.15*:* Sample placed on the descaling carriage which moves on the chain below the descaling nozzle

3.4.4 Analytical Techniques

After visual observation, descaled samples and removed scales were mounted in resin, and cross-sections polished for examination by scanning electron microscopy (SEM) in order to characterise the scale microstructure, composition and the metal-scale interfacial morphology. Scanning electron microscopy (SEM) observations were performed on a JSM-6300 scanning microscope. The specimens were mechanically polished using diamond paste, and some specimens were etched at room temperature for microstructure examination.

The average thickness of scale remaining on the descaled surfaces was found by means of image analysis (of SEM images). Energy-dispersive X-ray analysis (EDX) was used for point analyses of various phases in the scale.

X-ray diffraction (XRD) was used to identify scale and mould flux phases in contaminated and non contaminated samples. The target, voltage and current used were Co-Kα (Fe filter), 45kV and 40mA respectively.

Auger electron spectroscopy (AES) survey analyses were used to identify mould flux residues at the interface or in the scale. The beam voltage, beam current, tilt angle and the vacuum pressure used were 10kV, 10^{-6} A, 0° and 10^{-9} Torr, respectively. X-Ray photoelectron spectroscopy (XPS) survey, multiplex and deconvolution were used to determine the oxidation state of chromium in the removed scales.

X-ray fluorescence (XRF) and ICP-AES were used to analyse decarburized fluxes and scales after reheating. For XRF analysis, the oxide samples were ground to < 75µm in a tungsten carbide milling vessel, roasted at 1000°C to determine Loss On Ignition value and, after adding 1g sample to 6g $Li_2B_4O_7$, fused into bead. Major element analysis was executed on the fused bead using ARL9400XP + spectrometer. Another aliquot of the sample was pressed in a powder briquette for trace element analyses. Quantitative analyses of mould fluxes carbon and sulphur contents were done by means of LECO-Analysis.